



1 **Satellite Hydrology Observations as Operational Indicators of Forecasted** 2 **Fire Danger across the Contiguous United States**

3 Alireza Farahmand¹, E. Natasha Stavros¹, John T. Reager^{1*}, Ali Behrangi², James Randerson³,
4 Brad Quayle⁴

5 ¹ Jet Propulsion Laboratory, California Institute of Technology, Pasadena, CA

6 ² University of Arizona, Tucson, AZ

7 ³ University of California, Irvine

8 ⁴ USDA Forest Service Geospatial Technology and Applications Center, 2222 West 2300

9 SouthSalt Lake City, Utah 84119

10 * Corresponding Author

11

12 **Keywords:** wildfire; vapor pressure deficit (VPD); soil moisture; prediction; GRACE; AIRS

13 Abstract

14 Traditional methods for assessing fire danger often depend on meteorological forecasts, which
15 have reduced reliability after ~10 days. Recent studies have demonstrated long lead-time
16 correlations between pre-fire-season hydrological variables such as soil moisture and later fire
17 occurrence or area burned, yet no potential value of these relationships for operational forecasting
18 have not been studied. Here, we use soil moisture data refined by remote sensing observations of
19 terrestrial water storage from NASA's GRACE mission and vapor pressure deficit from NASA's
20 AIRS mission to generate monthly predictions of fire danger at scales commensurate with regional
21 management. We test the viability of predictors within nine US Geographic Area Coordination
22 Centers (GACCs) using regression models specific to each GACC. Results show that the model
23 framework improves interannual wildfire burned area prediction relative to climatology for all
24 GACCs. This demonstrates the importance of hydrological information to extend operational
25 forecast ability into the months preceding wildfire activity.

26 1. Introduction

27 Fires are a key disturbance globally, acting as a catalyst for terrestrial ecosystem change and
28 contributing significantly to both carbon emissions (Page et al., 2002) and changes in surface
29 albedo (Randerson et al., 2006). Furthermore, the socioeconomic impact of fires includes human
30 casualties as well as approximately \$21b loss in property from 1995-2015 (USD 2015;
31 NatCatSERVICE, accessed October 2017). Several studies have shown that in the Western US,
32 fires have demonstrated a positive trend in annual area burned that will likely continue into the
33 future (Littell et al., 2010; Stavros et al., 2014b). In response to increasing annual area burned and
34 detrimental losses, the US Forest Service has increased funding for active fire management from
35 16 to 52% of their total budget that would have otherwise been spent on land management and
36 research (USFS, 2015). These increased costs translate directly to increased USFS information



37 needs because any intra-or interannual early warning helps decrease the cost of preparing for,
38 managing, and, when necessary, suppressing fires that occur.

39 The severe consequences of wildfires motivate the need for capabilities to map fire potential on
40 timescales ranging from days to months. Operational fire management agencies rely on two
41 primary sources of information to predict fire danger: meteorological forecasts and expert
42 judgment (e.g. <https://www.predictiveservices.nifc.gov/outlooks/outlooks.htm>; accessed 28
43 November 20). Fire danger forecasts are generally reported in the form of qualitative categories
44 (e.g. normal, below-normal and above-normal). Such categories are used by the US National
45 Interagency Fire Center (NIFC) to allocate fire management resources across jurisdictional
46 boundaries (e.g., state or national) when local response capabilities are exhausted. These
47 qualitative metrics are derived from many information layers including fire danger indices.

48 Fire danger indices (e.g., the US National Fire Danger Rating System – NFDRS; Bradshaw et al.,
49 1983) typically use meteorological input (Abatzoglou & Brown, 2012; Holden & Jolly, 2011) that
50 is sometimes not available with the long-lead time needed for regional, transboundary fire
51 management planning. Gridded meteorological data often have several limitations. The data are
52 interpolated between weather stations (Daly et al., 2008), or developed by combing spatial and
53 temporal attributes of different climate data and validated with weather stations (Abatzoglou,
54 2013; Abatzoglou and Brown, 2012), or provided from meteorological reanalysis, i.e., numerical
55 weather prediction models that assimilate weather station data (Kalnay et al., 1996; Roads et al.,
56 1999). These weather stations are sometimes far removed from the location of interest, and are not
57 always good estimates of local climate, especially in complex topography. Moreover, forecasts
58 beyond 10 days for a given landscape location have low skill (Bauer et al., 2015). The mentioned
59 limitations of current operational fire danger systems result in the need for additional information
60 that could help improve predictions of fire danger at monthly intervals and to help allocate
61 resources across the country as the active fire season progresses and resources become strained.
62 This added information could result in less subjective and more accurate fire danger forecasts for
63 larger areas and for timescales of a month or longer.

64 A number of previous studies have demonstrated relationships between fire and hydrological
65 indicators (Parks et al., 2014; Shabbar et al., 2011; Westerling et al., 2002; Xiao and Zhuang,
66 2007). Vapor pressure deficit (VPD), specifically has been shown as an indicator of fire danger
67 (Abatzoglou and Williams, 2016; Seager et al., 2015; Williams et al., 2014) and is considered a
68 viable proxy for evapotranspiration demand and plant water stress during drought (Behrangi et al.,
69 2015; Weiss et al., 2012). VPD is defined as the amount of moisture in the air compared to amount
70 of moisture the air can hold. (Behrangi et al., 2016) shows that VPD in monthly time-scales has
71 the advantage in capturing onsets of meteorological droughts earlier than other variables such as
72 precipitation. This advantage could be helpful in developing fire-danger forecast models. More
73 recently, a study using model-assimilated observations of terrestrial water storage from NASA's
74 GRACE mission to assess pre-fire-season surface soil moisture conditions (January-April)
75 demonstrated skill in predicting both the number of fires and fire burned area in the following
76 May-April period (Jensen et al., 2017).

77 The goal of this work is to investigate the utility of remotely sensed hydrology observations for
78 predicting fire danger, defined as the amount of area likely to burn given an ignition, at spatial and
79 temporal scales commensurate with regional and global fire management decision-making.



80 Specifically, the objective is to investigate the utility of remotely sensed satellite-observed vapor
81 pressure deficit (VPD) from NASA's AIRS mission and surface soil moisture (SSM) from a
82 numerical data-assimilation of terrestrial water storage from NASA's GRACE mission as
83 indicators for predicting monthly fire danger across the United States from 2002 until 2016 at the
84 scale of the Geographic Area Coordination Centers (GACC) (**Figure 1**). To meet the objective,
85 we test the hypotheses that burned area varies monthly as a function of previous months' water
86 availability in the soil (SSM) and evaporative demand (i.e., previous months' VPD).

87 2. Methods

88 2.1. Datasets

89 For the purpose of this study, four input data sets were used (Figure 1):

- 90
- 91 1) Monthly VPD was generated from the AIRS near surface air temperature (T_{mean}) and relative
92 humidity (RH) Version 6 (Aumann et al., 2003; Goldberg et al., 2003). Please refer to (Behrangi
93 et al., 2016) for the formulation based on monthly air temperature (T_{mean}) and dewpoint
94 temperature (T_{dmean}) as well as the reliability of this formulation for monthly VPD derivation. The
95 data are in 0.5 degree spatial resolution and available since September 2002.
96
 - 97 2) Monthly surface soil moisture data were produced at the NASA Goddard Space Flight Center
98 (GSFC) using the Catchment Land Surface Model (CLSM) (a physically based land surface
99 model) and assimilated ground and space-based meteorological observations (Tapley et al., 2004;
100 Houborg et al., 2012; Reager et al., 2015; Zaitchik et al., 2008). The SSM data are available since
101 April 2004.
102
 - 103 3) The Global Fire Emissions Database version 4 (GFED-4s) provided wildfire burned area,
104 generated at 0.25 degree spatial resolution. GFED-4s is primarily derived from MODIS from 2001
105 to present and is reported as fraction of a cell burned for a given month (van der Werf et al., 2017).
106 GFED data are available since 1997. In this study, we have excluded agricultural fires by masking
107 out agricultural regions as classified by the 2011 National Landcover Database (NLCD 2011)
108 (Homer et al., 2015).
109

110 For consistency, all datasets were converted using linear interpolation into monthly, 0.25 degree
111 spatial resolution products that were then used to perform the model training and analysis for the
112 period 2003 through 2016.

113

114 2.2. Analysis

115 GACCs are geopolitical boundaries that represent similar fire-weather types and are used to
116 allocate fire management resources across the contiguous United States (CONUS) (Figure 1). In
117 this study, we predict anomalous monthly burned area using a linear regression model; a separate
118 model is developed for each GACC and for each month in a climatological sense. All fire events,
119 for a given GACC and a month of the year are selected as a single population for model training.
120 For example, all fires occurring in the Northern Rockies GACC, during the months of February
121 2004, February 2005, February 2006, etc. through February 2016 are placed into a single



122 population. Each monthly, 0.25 degree fire burned area observation has a matched SSM and VPD
 123 observation at the corresponding time and grid location. These sets are then used to train the model,
 124 and various time lags are imposed between the independent variables (SSM and VPD) and the
 125 dependent variable (burned area) in order to maximize predictive skill.

126 Each GACC uses the “best” prior VPD-SSM combination for all months. The “best” model was
 127 identified for each GACC by selecting the lagged model with the highest Weighted Nash-Sutcliffe
 128 efficiency (E_w):

$$129 \quad E_w = \sum_{j=1}^{12} E_j * FAB_j$$

130 where FAB_j is the mean historical fraction of annual area burned in month j , and E_j is the Nash-
 131 Sutcliffe (E) for any given month (j). E_j (Nash and Sutcliffe, 1970) is a metric that measures the
 132 skill of the model against the skill of the long term mean value (i.e. persistence), defined as:

$$133 \quad E_j = 1 - \frac{\sum_{i=1}^n (AB_{obs,i} - AB_s)^2}{\sum_{i=1}^n (AB_{obs,i} - AB_c)^2}$$

134 where n is total number of observations, X_{obs} is observed area burned in month j and AB_s is the
 135 model simulated area burned for month j , and AB_c is the mean area burned in month j over the
 136 climatological record. E can range between $-\infty$ and 1. E of zero shows that the model performance
 137 is as good as the mean of observations over the entire record. If E exceeds 0, the model performs
 138 better than the mean of observations and if E falls below zero, the mean of observations is a better
 139 predictor than the model simulations. An E of 1 represents the perfect prediction by the model.

140 We constructed a forecasting method that would only rely on the model prediction of burned area,
 141 as opposed to the burned area climatology, if the model had demonstrated skill for a given month.
 142 The estimation of E_w for each GACC and for each monthly model ensures that months with higher
 143 predictive skill are assigned a higher weight in the combined time series. Also, months exhibiting
 144 higher amount of historical wildfire activity are assigned a higher weight as well.

145 The model is then defined as follows:

$$146 \quad AB_s = AB_c + AB_A, \text{ where } AB_A = a + b * (VPD_A) + c * (SSM_A) \text{ if } E_j > 0$$

$$147 \quad AB_A = 0 \text{ if } E_j \leq 0$$

148 AB_s is the simulated area burned for a given month, AB_c is the climatological area burned or the
 149 mean annual area burned by month, VPD_A and SSM_A are the anomalous VPD and SSM in one,
 150 two or three months prior to the wildfire month. Different combinations of prior VPD and SSM
 151 observations were tested to represent the reliability of a single VPD-SSM model per GACC for
 152 the entire year.

153 Finally, AB_s is compared to AB_c by comparing two Nash-Sutcliffe (E) values of the entire time
 154 series. The first E is measured using the 2003-2016 monthly time series of model predictions and
 155 observations ($E_{\text{simulated,observation}}$). The second E is computed by using 2003-2016 monthly time



156 series of climatology and observations ($E_{\text{climatology, observation}}$). If $E_{\text{simulated, observation}}$ exceeds $E_{\text{climatology, observation}}$,
157 $E_{\text{climatology, observation}}$, the model has more accuracy compared to the climatology. If $E_{\text{climatology, observation}}$
158 is greater than $E_{\text{simulated, observation}}$, then the climatology has more accuracy in forecasting wildfire
159 activity.

160 Results

161 Figure 2 shows the hydrologic variable combination used to develop the best model of anomaly
162 burned area using the monthly Nash-Sutcliffe (E), the weighted Nash-Sutcliffe (E_w), and the
163 fraction of annual area burned for each month, while Table 1 shows the best variable combination
164 for each GACC. There are some notable patterns, though few without exceptions. For example,
165 Northern California, Northern Rockies and the Northwest all have the same peak month (August)
166 for area burned, while also having significant fractions of evergreen (Figure 1). Area burned in the
167 Great Basin also peaks in August, however it does not have substantial evergreen landcover,
168 although at this spatial scale we can not determine if that is where fires happen. The models with
169 the highest relative predictive ability throughout the year (denoted by weighted Nash- Sutcliffe)
170 are generally in the GACCs with substantial landcover and dominated by fuel limited systems
171 (herbaceous and shrublands): Great Basin, Southern California, Rocky Mountains, Northwest,
172 Northern Rockies; however, the Southwest also has heavy herbaceous, but has relative low
173 predictability throughout the year. Similarly, the Northern Rockies, Northwest, Rocky Mountains
174 and Great Basin all have high predictability in their peak burned area month and are all
175 substantially covered by herbaceous, but the Southwest does not. One pattern that is robust is that
176 the Great Basin, the Southwest, and Southern California all rely on 1-month lead soil moisture in
177 their predictive model and all also have substantial shrubland cover. Notably, the Eastern, Northern
178 Rockies, Rocky Mountains, Southern California and Southern GACCs all have bimodal burned
179 area distributions, but no similar landcover characteristics to explain the pattern.

180 Figure 3 shows two example cases of model predictions based on hydrological variables. We show
181 results for our best and worst performing GACC in order to capture the range of model skill in
182 different fire climate regions. For our best performing GACC, the Northern Rockies, we see
183 consistent peaks in between dominant hydrologic variable, VPD and the fire area burned,
184 suggesting the dominant role of VPD in fire burned area prediction for that GACC (Table 1). These
185 strong relationships between hydrology and wildfire occurrence in the Northern Rockies confirms
186 the findings of the previous studies (Littell et al., 2009; Westerling et al., 2011). For our worst
187 performing GACC, the Southern, two hydrologic variables are seemingly much more connected
188 and it is less clear what drives the pattern of monthly area burned.

189 In order to evaluate the model predictions against the observations, we have calculated two Nash-
190 Sutcliffe coefficients (Table 1). As shown, for all GACCs, the model is forecasting the wildfire
191 activity with higher accuracy than the climatology, but the improvement is variable by GACC.
192 The results reveal that the Rocky Mountains and Northern Rockies GACCs have the best model
193 performance (E of 0.82 and 0.64 respectively), while the Southwest and Southern CA (E of 0.34
194 and 0.35 respectively) show the least model performance. Similar to the time series of the Eastern
195 and Southern GACCs, the model has not improved the climatology to a great extent. In all other
196 regions, the improvement of the simulated compared to the climatology is substantial. The key



197 difference between overall evaluation metric ($E_{S,c}$) and the time series is that the time series
198 demonstrate the variability of predictive ability from month to month.

199 Figure 4 shows the time series of wildfire burned area observation (blue), simulation (red) and
200 climatology (yellow) for nine different GACCs from 2003 through 2016. This figure shows that
201 the performance of the model varies by location and months. In general, the models capture
202 interannual variability for most GACCs. Notably in Figure 4, some months show the simulation
203 has higher agreement to the observations than does the climatology. In the Southern GACCs,
204 model performance is relatively similar to the climatology. In the Southern GACC, both the
205 simulation and climatology indicate close agreement with the observations. In the Northern
206 Rockies and Rocky Mountains show the highest agreement between model and observations in
207 the higher than normal fire years. Specifically, in the Northern Rockies, the model detects expected
208 burned area for the above-than normal fire activity years 2003, 2006, 2007 and 2012; and in the
209 Rocky Mountains GACC, years 2006, 2008, 2009, 2011, 2015 and 2016 show high agreement
210 between simulated and the observations. The model also detects higher than normal fire activity
211 in Northern California years 2012, 2014 and 2015, Northwest years 2006, 2007, 2012, 2014 and
212 2015, Great basin years 2006, 2007, 2012 and 2013, and Eastern for years 2004, 2012 for Eastern
213 GACC. Lastly, the simulation outperforms the climatology slightly for Southern CA and the
214 Southwest. However, neither model nor the climatology have detected inter-annual fire activity
215 for these regions with high accuracy.

216 Lastly, the models were built using only either VPD or SSM to determine the relative influence of
217 either variable on burned area within each GAAC (Table 1, $E_{S,VPD}$ and $E_{S,SSM}$). For some of the
218 GAACs, the influence of the variable appears to be associated with the relative fractions of
219 landcover influenced by that variable. For example, in the Northern Rockies, it is roughly half
220 evergreen forest and half herbaceous (Figure 1); evergreen forest typically need to be dried to
221 sustain combustion (high VPD in the month prior), while herbaceous communities typically need
222 wet conditions months prior to grow fuels (high SSM 2 months prior). Similarly, in the Northwest
223 it is roughly half evergreen (high VPD two months prior) and half shrub (high SSM three months
224 prior). The Rocky Mountains are mostly herbaceous and shrubland (high SSM three months prior)
225 but has some evergreen (high VPD one month prior). In Northern California, landcover is mostly
226 evergreen (high VPD one month prior) with some shrub (high soil moisture two months prior).
227 The other GAACs have less obvious relationships between landcover and hydrology.

228 Discussion and Conclusion

229 Wildfire activity results in billions of dollars of losses every year (USD 2015; NatCatSERVICE,
230 accessed October 2017). Forecasting wildfire activity could therefore substantially reduce the
231 damages associated with wildfire burned area. Historical wildfire prediction models have
232 limitations including the mismatch in scale between fire danger models and common application,
233 as well as the unreliability of meteorological data in remote regions. As such, current operational
234 wildfire forecast models for forecasts >10 days are heavily based on subjective expert knowledge
235 to predict expected area burned. Thus, the aim of this study was to predict area burned in different
236 geographic regions (GACCs) of the United States.



237 There are some notable patterns in predictive model development across GACCs largely driven
238 by landcover fractional cover and mesoscale climate (Table 1). The Great Basin, the Southwest,
239 and Southern California GACCs all have substantial shrubland cover and have the same soil
240 moisture predictor (1-month lead). This could be a function of the shallow rooting of shrubs. This
241 was the only pattern by landcover that was not contradicted by mesoscale climatic influence. For
242 example, the Great Basin, Southern California, Rocky Mountains, Northwest, and Northern
243 Rockies models have the highest predictive ability throughout the year (E_w) and have substantial
244 landcover dominated by fuel-limited systems (grasslands and shrublands). Fuel limited systems
245 typically rely on pre-fire season conditions to grow fuels that carry fire, thus influencing the total
246 burned area (Stavros et al., 2014a; Swetnam and Betancourt, 1998). Although the Southwest also
247 has heavy grasslands, it has a relatively low predictability throughout the year, but is the GACC
248 most influenced by the Southwest Monsoon, which can have variable onset that affects the fire
249 season (Grissino Mayer and Swetnam, 2000). The southwest monsoon also explains why the
250 Northern Rockies, Northwest, Rocky Mountains and Great Basin all have high predictability in
251 their peak burned area month, but the Southwest (also substantially covered by grasslands) does
252 not. Further substantiating the claim that mesoscale climate affects model predictability is the fact
253 that Southern California has a bimodal distribution of fire area burned throughout the year.
254 According to (Jin et al., 2014), there are two different kinds of fire in Southern California (those
255 in the summer driven by hot and dry conditions and those in the fall driven by Santa Ana winds)
256 and each have different climatic conditions explaining the number of fires and burned area.

257 Beyond climate and landcover, humans play a significant role in the predictability of area burned
258 (Balch et al., 2017). This explains the bimodal fire distributions found in the Eastern, Northern
259 Rockies, Rocky Mountains, and Southern GACCs. Most of the fires in the Eastern and Southern
260 GACCs are prescribed burns, which can happen throughout the year (as denoted by the relatively
261 flat, although slight bimodal distributions of percent annual area burned by month – Table 1). Also,
262 there is a notable decoupling of the relationship between hydrologic variables and burned area
263 (Figure 4) in the Southern GAAC, which has mostly anthropogenic fire starts, as compared to the
264 Northern Rockies, which has mostly lightning caused ignitions when burned area peaks in Fall
265 (Figure 2). This also explains why the simulation performs closely to the climatology (Figure 3),
266 with only minor improvements in Nash-Sutcliffe as compared to other GACCs (Table 1). Notably,
267 the GAACs that have a strong bimodal distribution perform less well than those that don't,
268 however in all GAACs with bimodal distributions (Figure 2), there are substantial crop lands
269 (which were excluded from the analysis) where agricultural burning occurs independent of the
270 hydrologic conditions (Figure 1).

271 Mesoscale climate (e.g., monsoons) and anthropogenic influence on fire regimes, are likely less
272 direct relationships between hydrologic variables and burned area. Specifically, the GACCs that
273 are more influenced by mesoscale climate (Southern California and the Southwest) and by
274 anthropogenic burning (Southern and Eastern) did not show a clear association between relative
275 influence of the hydrologic variable and the relative fractions of landcover, unlike the Northern
276 Rockies, Northwest, Northern California or Rocky Mountains.

277 In general, this work demonstrates how lead data on hydrologic variables that can be measured by
278 satellite (i.e., not limited by proximity to in situ infrastructures) can be used to forecast fire danger
279 1-month before it happens. In all geographic regions, the models improved over normal (Table 2)
280 and demonstrated the ability to capture interannual variability (Figure 2). Future work should



281 consider how these models are developed by landcover type and if there are different models based
282 on how that landcover type is typically managed (e.g., cropland vs. forest).

283 Acknowledgements

284 The data used for this study is freely available at:

285 Vapor Pressure Deficit (VPD): https://airs.jpl.nasa.gov/data/get_data

286 Surface Soil Moisture (SSM): <https://nasagrace.unl.edu/>

287 Fire Burned Area: <https://www.globalfiredata.org/data.html>

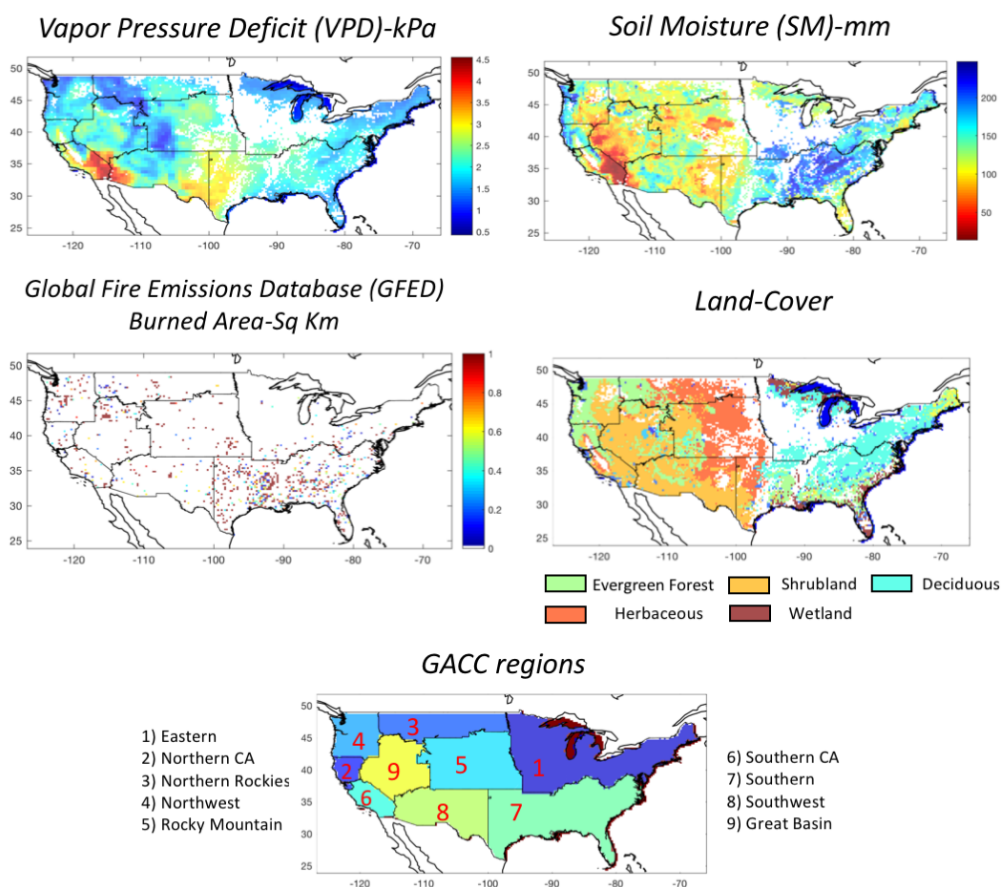
288 Land-cover map: https://www.mrlc.gov/nlcd11_data.php

289 We would like to acknowledge Ed Delgado, at National Interagency Fire Center (NIFC). This
290 research was carried out at the Jet Propulsion Laboratory, California Institute of Technology, under
291 a contract with the National Aeronautics and Space Administration (NASA). This research was
292 supported by Jet Propulsion Laboratory research and technological development program in Earth
293 Sciences.

294

295

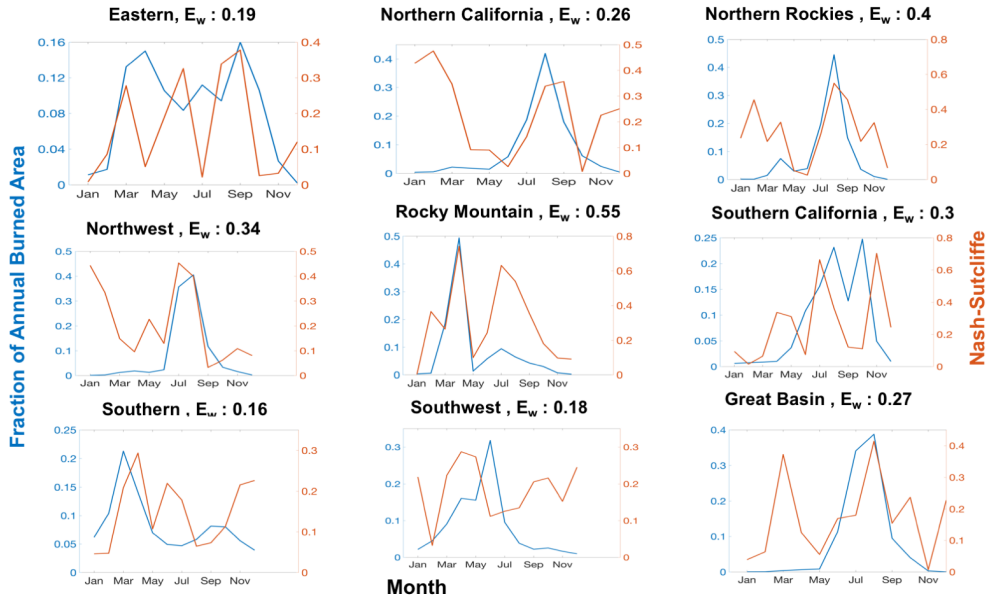
296



297

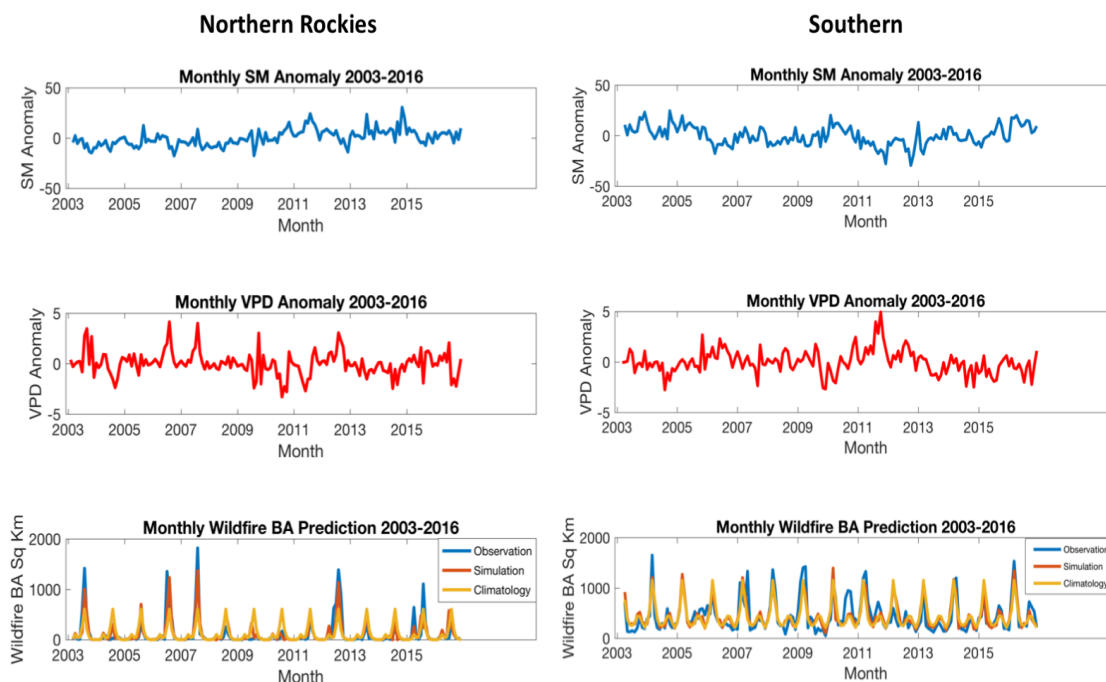
298 Figure 1: Snapshot of August 2010 of the datasets used in relation to the Geographic Area
 299 Coordination Centers (GACCs).

300



301
 302
 303
 304
 305
 306
 307
 308

Figure 2. Model selection based on the monthly Nash-Sutcliffe for each GACC. The blue line shows variable peak fire month by mean annual area burned (FAB) and the orange line shows the monthly Nash-Sutcliffe for each GACC showing variable peak fire month. The weighted Nash-Sutcliffe is calculated using the different combinations of VPD and SSM. The best model was selected based on highest E_w , which demonstrates the relative strength of the different models by GACC.



309
310 Figure 3. The impact of hydrologic predictors on best and worst performing Geographic Area
311 Coordination Centers (GACCs) models. Monthly time series from 2003 through 2016 show the
312 GACCs with the best (left) and worst (right) coupled response of burned area (bottom) to vapor
313 pressure deficit anomaly (middle) and soil moisture anomaly (top); thus, demonstrating the
314 respective value added of these variables in the modeled burned area (“simulation” in orange)
315 compared to the climatology (yellow) as compared to the observed (blue).
316



317
318
319
320
321
322
323
324
325
326
327
328
329
330
331
332
333
334
335
336
337
338
339
340
341

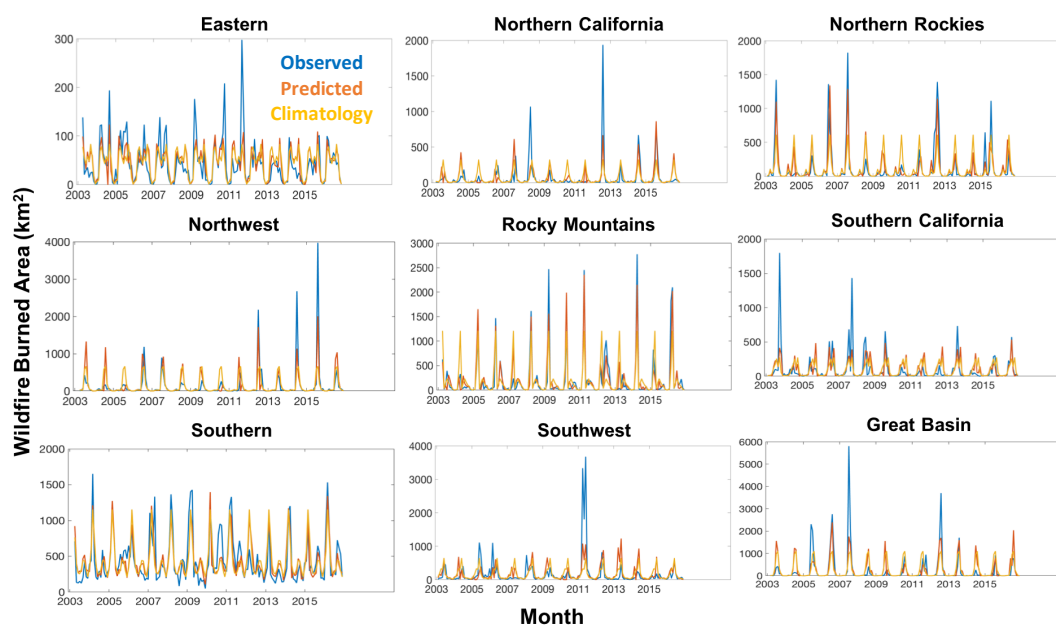


Figure 4. The ability of the regional models to predict (orange) the observed burned area (blue) is improved over the climatology (yellow), which demonstrates the ability to capture interannual variability by Geographic Area Coordination Centers.



GACC	AB_A =	E_S	E_C	E_S - E_C	E_{S, VPD}	E_{S, ssm}
Eastern	VPD ₋₂ + SSM ₋₃	0.51	0.37	0.14	0.42	0.42
Northern California	VPD ₋₁ + SSM ₋₂	0.44	0.22	0.22	0.29	0.33
Northern Rockies	VPD ₋₁ + SSM ₋₂	0.64	0.38	0.26	0.63	0.39
Northwest	VPD ₋₂ + SSM ₋₃	0.58	0.28	0.30	0.46	0.42
Rocky Mountains	VPD ₋₁ + SSM ₋₃	0.82	0.51	0.31	0.64	0.61
Southern California	VPD ₋₁ + SSM ₋₁	0.35	0.19	0.16	0.25	0.29
Southern	VPD ₋₂ + SSM ₋₃	0.64	0.57	0.07	0.63	0.59
Southwest	VPD ₋₁ + SSM ₋₁	0.34	0.16	0.18	0.28	0.23
Great Basin	VPD ₋₂ + SSM ₋₁	0.47	0.3	0.17	0.43	0.37

342

343 Table 1. Overall model performance and separate influence of individual hydrologic variables. We
 344 use Nash-Sutcliffe coefficients to describe the combined Soil Moisture (SSM) and Vapor Pressure
 345 Deficit (VPD) simulation performance (E_S), the climatology performance (E_C) and the individual
 346 predictor performance (E_{S, VPD}, E_{S, ssm}) vs the observations. All Geographic Area Coordination
 347 Centers show improved performance (E_S - E_C) on the VPD and SM combined model for Area
 348 Burned (AB_A). Either SM or VPD improve the prediction, but not as much as the combined model.

349

350

351 References

- 352 Abatzoglou, J. T.: Development of gridded surface meteorological data for ecological
 353 applications and modelling, *Int. J. Climatol.*, 33(1), 121–131, doi:10.1002/joc.3413, 2013.
- 354 Abatzoglou, J. T. and Brown, T. J.: A comparison of statistical downscaling methods suited for
 355 wildfire applications, *Int. J. Climatol.*, 32(5), 772–780, doi:10.1002/joc.2312, 2012.
- 356 Abatzoglou, J. T. and Williams, A. P.: Impact of anthropogenic climate change on wildfire
 357 across western US forests., *Proc. Natl. Acad. Sci. U. S. A.*, 113(42), 11770–11775,
 358 doi:10.1073/pnas.1607171113, 2016.
- 359 Aumann, H. H., Chahine, M. T., Gautier, C., Goldberg, M. D., Kalnay, E., McMillin, L. M.,
 360 Revercomb, H., Rosenkranz, P. W., Smith, W. L., Staelin, D. H., Strow, L. L. and Susskind, J.:
 361 AIRS/AMSU/HSB on the aqua mission: design, science objectives, data products, and
 362 processing systems, *IEEE Trans. Geosci. Remote Sens.*, 41(2), 253–264,
 363 doi:10.1109/TGRS.2002.808356, 2003.
- 364 Balch, J. K., Bradley, B. A., Abatzoglou, J. T., Nagy, R. C., Fusco, E. J. and Mahood, A. L.:
 365 Human-started wildfires expand the fire niche across the United States, *Proc. Natl. Acad. Sci.*,
 366 114(11), 2946–2951, doi:10.1073/pnas.1617394114, 2017.



- 367 Bauer, P., Thorpe, A. and Brunet, G.: The quiet revolution of numerical weather prediction,
368 *Nature*, 525(7567), 47–55, doi:10.1038/nature14956, 2015.
- 369 Behrangi, A., Loikith, P., Fetzer, E., Nguyen, H. and Granger, S.: Utilizing Humidity and
370 Temperature Data to Advance Monitoring and Prediction of Meteorological Drought, *Climate*,
371 3(4), 999–1017, doi:10.3390/cli3040999, 2015.
- 372 Behrangi, A., Fetzer, E. J. and Granger, S. L.: Early detection of drought onset using near surface
373 temperature and humidity observed from space, *Int. J. Remote Sens.*, 37(16), 3911–3923,
374 doi:10.1080/01431161.2016.1204478, 2016.
- 375 Bradshaw, L. S., Deeming, J. E., Burgan, R. E. and Cohen, J. D.: The National Fire-Danger
376 Rating System--1978., 1983.
- 377 Daly, C., Halbleib, M., Smith, J. I., Gibson, W. P., Doggett, M. K., Taylor, G. H., Curtis, J.,
378 Pasteris, P. P. and Curtis, J.: Physiographically sensitive mapping of climatological temperature
379 and precipitation across the conterminous United States, *Int. J. Climatol.*, 28(15), 2031–2064,
380 doi:10.1002/joc.1688, 2008.
- 381 Goldberg, M. D., Yanni Qu, McMillin, L. M., Wolf, W., Lihang Zhou and Divakarla, M.: AIRS
382 near-real-time products and algorithms in support of operational numerical weather prediction,
383 *IEEE Trans. Geosci. Remote Sens.*, 41(2), 379–389, doi:10.1109/TGRS.2002.808307, 2003.
- 384 Grissino Mayer, H. D. and Swetnam, T. W.: Century scale climate forcing of fire regimes in the
385 American Southwest, *The Holocene*, 10(2), 213–220, doi:10.1191/095968300668451235, 2000.
- 386 Holden, Z. A. and Jolly, W. M.: Modeling topographic influences on fuel moisture and fire
387 danger in complex terrain to improve wildland fire management decision support, *For. Ecol.*
388 *Manag.*, 262(12), 2133–2141, doi:10.1016/j.foreco.2011.08.002, 2011.
- 389 Homer, C., Dewitz, J., Yang, L., Jin, S., Danielson, P., Xian, G., Coulston, J., Herold, N.,
390 Wickham, J. and Megown, K.: Completion of the 2011 National Land Cover Database for the
391 conterminous United States—representing a decade of land cover change information,
392 *Photogramm. Eng. Remote Sens.*, 81(5), 345–354, 2015.
- 393 Houborg, R., Rodell, M., Li, B., Reichle, R. and Zaitchik, B. F.: Drought indicators based on
394 model-assimilated Gravity Recovery and Climate Experiment (GRACE) terrestrial water storage
395 observations: GRACE-BASED DROUGHT INDICATORS, *Water Resour. Res.*, 48(7),
396 doi:10.1029/2011WR011291, 2012.
- 397 Jensen, D., Reager, J., Zajic, B., Rousseau, N., Rodell, M. and Hinkley, E.: The sensitivity of US
398 wildfire occurrence to pre-season soil moisture conditions across ecosystems, *Environ. Res.*
399 *Let.*, doi:10.1088/1748-9326/aa9853, 2017.
- 400 Jin, Y., Randerson, J. T., Faivre, N., Capps, S., Hall, A. and Goulden, M. L.: Contrasting controls
401 on wildland fires in Southern California during periods with and without Santa Ana winds:
402 Controls on Southern California fires, *J. Geophys. Res. Biogeosciences*, 119(3), 432–450,
403 doi:10.1002/2013JG002541, 2014.



- 404 Kalnay, E., Kanamitsu, M., Kistler, R., Collins, W., Deaven, D., Gandin, L., Iredell, M., Saha,
405 S., White, G., Woollen, J., Zhu, Y., Leetmaa, A., Reynolds, R., Chelliah, M., Ebisuzaki, W.,
406 Higgins, W., Janowiak, J., Mo, K. C., Ropelewski, C., Wang, J., Jenne, R. and Joseph, D.: The
407 NCEP/NCAR 40-Year Reanalysis Project, *Bull. Am. Meteorol. Soc.*, 77(3), 437–471,
408 doi:10.1175/1520-0477(1996)077<0437:TNYRP>2.0.CO;2, 1996.
- 409 Littell, J. S., McKenzie, D., Peterson, D. L. and Westerling, A. L.: Climate and wildfire area
410 burned in western U.S. ecoprovinces, 1916–2003, *Ecol. Appl.*, 19(4), 1003–1021,
411 doi:10.1890/07-1183.1, 2009.
- 412 Littell, J. S., Oneil, E. E., McKenzie, D., Hicke, J. A., Lutz, J. A., Norheim, R. a. and Elsner, M.
413 M.: Forest ecosystems, disturbance, and climatic change in Washington State, USA, *Clim.
414 Change*, 102(1–2), 129–158, doi:10.1007/s10584-010-9858-x, 2010.
- 415 Nash, J. E. and Sutcliffe, J. V.: River flow forecasting through conceptual models part I — A
416 discussion of principles, *J. Hydrol.*, 10(3), 282–290, doi:10.1016/0022-1694(70)90255-6, 1970.
- 417 Page, S. E., Siegert, F., Rieley, J. O., Boehm, H.-D. V., Jaya, A. and Limin, S.: The amount of
418 carbon released from peat and forest fires in Indonesia during 1997, *Nature*, 420(November), 61–
419 65, doi:10.1038/nature01141.1, 2002.
- 420 Parks, S. A., Parisien, M.-A., Miller, C. and Dobrowski, S. Z.: Fire Activity and Severity in the
421 Western US Vary along Proxy Gradients Representing Fuel Amount and Fuel Moisture, edited
422 by M. Germino, *PLoS ONE*, 9(6), e99699, doi:10.1371/journal.pone.0099699, 2014.
- 423 Randerson, J. T., Liu, H., Flanner, M. G., Chambers, S. D., Jin, Y., Hess, P. G., Pfister, G.,
424 Mack, M. C., Treseder, K. K., Welp, L. R., Chapin, F. S., Harden, J. W., Goulden, M. L., Lyons,
425 E., Neff, J. C., Schuur, E. A. G. and Zender, C. S.: The impact of boreal forest fire on climate
426 warming., *Science*, 314(5802), 1130–2, doi:10.1126/science.1132075, 2006.
- 427 Reager, J., Thomas, A., Sproles, E., Rodell, M., Beaudoin, H., Li, B. and Famiglietti, J.:
428 Assimilation of GRACE Terrestrial Water Storage Observations into a Land Surface Model for
429 the Assessment of Regional Flood Potential, *Remote Sens.*, 7(11), 14663–14679,
430 doi:10.3390/rs71114663, 2015.
- 431 Roads, J. O., Chen, S.-C., Kanamitsu, M. and Juang, H.: Surface water characteristics in NCEP
432 global spectral model and reanalysis, *J. Geophys. Res. Atmospheres*, 104(D16), 19307–19327,
433 doi:10.1029/98JD01166, 1999.
- 434 Seager, R., Hooks, A., Williams, A. P., Cook, B., Nakamura, J. and Henderson, N.: Climatology,
435 variability, and trends in the U.S. Vapor pressure deficit, an important fire-related meteorological
436 quantity, *J. Appl. Meteorol. Climatol.*, 54(6), 1121–1141, doi:10.1175/JAMC-D-14-0321.1,
437 2015.
- 438 Shabbar, A., Skinner, W. and Flannigan, M. D.: Prediction of Seasonal Forest Fire Severity in
439 Canada from Large-Scale Climate Patterns, *J. Appl. Meteorol. Climatol.*, 50(4), 785–799,
440 doi:10.1175/2010JAMC2547.1, 2011.



- 441 Stavros, E. N., Abatzoglou, J., Larkin, N. K., McKenzie, D. and Steel, E. A.: Climate and very
442 large wildland fires in the contiguous western USA, *Int. J. Wildland Fire*, 23(7), 899,
443 doi:10.1071/WF13169, 2014a.
- 444 Stavros, E. N., Abatzoglou, J. T., McKenzie, D. and Larkin, N. K.: Regional projections of the
445 likelihood of very large wildland fires under a changing climate in the contiguous Western
446 United States, *Clim. Change*, 126(3–4), 455–468, doi:10.1007/s10584-014-1229-6, 2014b.
- 447 Swetnam, T. W. and Betancourt, J. L.: Mesoscale Disturbance and Ecological Response to
448 Decadal Climatic Variability in the American Southwest, *J. Clim.*, 11(12), 3128–3147,
449 doi:10.1175/1520-0442(1998)011<3128:MDAERT>2.0.CO;2, 1998.
- 450 USFS: The Rising Cost of Wildfire Operations: Effects on the Forest Service’s Non-Fire Work.,
451 2015.
- 452 Weiss, J. L., Betancourt, J. L. and Overpeck, J. T.: Climatic limits on foliar growth during major
453 droughts in the southwestern USA: GROWTH LIMITS DURING SOUTHWEST DROUGHTS,
454 *J. Geophys. Res. Biogeosciences*, 117(G3), n/a-n/a, doi:10.1029/2012JG001993, 2012.
- 455 van der Werf, G. R., Randerson, J. T., Giglio, L., van Leeuwen, T. T., Chen, Y., Rogers, B. M.,
456 Mu, M., van Marle, M. J. E., Morton, D. C., Collatz, G. J., Yokelson, R. J. and Kasibhatla, P. S.:
457 Global fire emissions estimates during 1997–2016, *Earth Syst. Sci. Data*, 9(2), 697–720,
458 doi:10.5194/essd-9-697-2017, 2017.
- 459 Westerling, A. L., Gershunov, A., Cayan, D. R. and Barnett, T. P.: Long lead statistical forecasts
460 of area burned in western U.S. wildfires by ecosystem province, *Int. J. Wildland Fire*, 11(4), 257,
461 doi:10.1071/WF02009, 2002.
- 462 Westerling, A. L., Turner, M. G., Smithwick, E. A. H., Romme, W. H. and Ryan, M. G.:
463 Continued warming could transform Greater Yellowstone fire regimes by mid-21st century,
464 *Proc. Natl. Acad. Sci.*, 108(32), 13165–13170, doi:10.1073/pnas.1110199108, 2011.
- 465 Williams, A. P., Seager, R., Macalady, A. K., Berkelhammer, M., Crimmins, M. A., Swetnam, T.
466 W., Trugman, A. T., Buening, N., Noone, D., McDowell, N. G., Hryniw, N., Mora, C. I. and
467 Rahn, T.: Correlations between components of the water balance and burned area reveal new
468 insights for predicting forest fire area in the southwest United States, *Int. J. Wildland Fire*, 24(1),
469 14–26, 2014.
- 470 Xiao, J. and Zhuang, Q.: Drought effects on large fire activity in Canadian and Alaskan forests,
471 *Environ. Res. Lett.*, 2(4), 044003, doi:10.1088/1748-9326/2/4/044003, 2007.
- 472 Zaitchik, B. F., Rodell, M. and Reichle, R. H.: Assimilation of GRACE Terrestrial Water
473 Storage Data into a Land Surface Model: Results for the Mississippi River Basin, *J.*
474 *Hydrometeorol.*, 9(3), 535–548, doi:10.1175/2007JHM951.1, 2008.
- 475